2010 American Control Conference
Marriott Waterfront, Baltimore, MD, USA
June 30-July 02, 2010

Active and Passive Fault-Tolerant LPV Control of Wind Turbines

Christoffer Sloth, Thomas Esbensen, and Jakob Stoustrup

Abstract— **This paper addresses the design and comparison of active and passive fault-tolerant linear parameter-varying (LPV) controllers for wind turbines. The considered wind turbine plant model is characterized by parameter variations along the nominal operating trajectory and includes a model of an incipient fault in the pitch system. We propose the design of an active fault-tolerant controller (AFTC) based on an existing LPV controller design method and extend this method to apply for the design of a passive fault-tolerant controller (PFTC).**

Both controllers are based on output feedback and are scheduled on the varying parameter to manage the parameter-varying nature of the model. The PFTC only relies on measured system variables and an estimated wind speed, while the AFTC also relies on information from a fault diagnosis system. Consequently, the optimization problem involved in designing the PFTC is more difficult to solve, as it involves solving bilinear matrix inequalities (BMIs) instead of linear matrix inequalities (LMIs).

Simulation results show the performance of the active fault-tolerant control system to be slightly superior to that of the passive fault-tolerant control system.

I. INTRODUCTION

Among the renewable energy sources available today, wind energy is the world's fastest growing with an annual growth in installed capacity of 30% on average throughout the past 10 years [1]. As many wind turbines are installed offshore, unscheduled service can be highly costly, so it would be beneficial if fault-tolerant control schemes could help the wind turbines to maintain power production from the time a fault occurs to the next scheduled service.

In this paper a three-bladed horizontal-axis variable-speed wind turbine is considered. The aerodynamic properties of the wind turbine are functions of the pitch angles of the blades, the speed of the rotor, and the wind speed. The wind exerts torque and thrust on the rotor. The aerodynamic torque is transferred to the generator through a drive train, which multiplies the rotor's rotational speed. The aerodynamic thrust is transferred to the tower-top.

In terms of control, the wind turbine works in two distinct regions. Below a certain wind speed, in the partial load region, the turbine is controlled to generate as much power as possible. This is achieved by adjusting the generator torque to obtain an optimum ratio between the tip speed of the blades and the wind speed. In the full load region, the wind turbine is controlled to produce a rated power output at a constant rotor speed, which is obtained by pitching the blades to adjust the efficiency of the rotor, while applying a constant generator torque. In this paper only operation in the full load region is considered.

Due to the varying dynamic behavior of wind turbines along their nominal operating trajectory, wind turbine controllers typically consist of multiple gain-scheduled controllers, which are designed to operate in the proximity of a certain operating point. In [2] this is shown for classical controllers and in [3][4] by introducing bumpless transfer between robust controllers. The underlying assumption for such control schemes is that the parameters will only change slowly compared to the system dynamics, which is generally not satisfied. Additionally, classic gain-scheduling controllers only ensure performance guarantees and stability at the operating points where the linear controllers are designed.

A systematic way of designing parameter-dependent controllers is within the framework of linear parameter-varying (LPV) control. Here, a controller is synthesized to satisfy a performance specification for all possible parameter values within a specified model and for the specified rate of variation of the parameters. The controller can be synthesized after solving an optimization problem subject to linear matrix inequalities (LMIs).

In previous work, LPV controllers have been developed for wind turbines considering a nominal plant model [5][6]. In this paper however, LPV controllers are designed to be tolerant against a specified set of faults combined with the capability of dealing with the parameter-varying nature of the wind turbine model. In order to compare the differences in terms of design complexity and performance, both an active fault-tolerant controller (AFTC) and a passive fault-tolerant controller (PFTC) are considered in this paper.

The difference between an AFTC and a PFTC is that an active fault-tolerant controller relies on a fault diagnosis system, which should feed information about the faults to the controller. This knowledge makes it possible for the AFTC to reconfigure according to the current state of the system, but it also introduces a risk of false positive and false negative diagnosis, e.g. due to model errors. The PFTC has no risk of making false decisions and has no detection time either. Conversely, it is not necessarily optimal at any given time, since some conservatism is introduced in its design, also for the nominal situation. The PFTC is optimized for the fault-free situation, while satisfying some degraded performance requirements in the fault scenario. The degradation of requirements is what separates reliable controllers from robust controllers, which have the same performance guarantee in the entire parameter space.

To focus primarily on the design and synthesis methods, this paper addresses the simple case of a single fault: altered

Christoffer Sloth, Thomas Esbensen, and Jakob Stoustrup have carried out the work at Automation and Control, Department of Electronic Systems, Aalborg University, DK-9220 Aalborg East, Denmark

dynamics of the hydraulic pitch system due to high air content in the hydraulic oil. The motivation for considering this fault, and the modeling of it, originates from [7]. For a more comprehensive treatment of multiple fault types related to wind turbine operation see [8].

This paper is organized as follows: Section II describes the wind turbine plant model and the considered fault. In Section III the optimization problems and controller synthesis procedures are presented for designing the active and passive fault-tolerant LPV controllers. Section IV contains the simulation results and compares the performance of the fault-tolerant controllers to that of a reference controller. Section V concludes the paper.

II. WIND TURBINE MODEL

A non-linear wind turbine model is used for simulation of the proposed control algorithms. The model consists of a static aerodynamic model, a tower model, a two-mass model of the drive train, a model of the generator, actuator models, and measurement noise. Additional information about the model is found in [8].

A. Aerodynamic Model

The rotor of the wind turbine converts energy from the wind to the rotor shaft, rotating at the speed $\omega_{\mathrm{r}}(t)$. The power in the wind depends on the wind speed, $v_{\mathrm{r}}(t)$, the air density, ρ, and the swept area, A. From the available power in the swept area, the power transferred to the rotor is given based on the power coefficient, $C_{\mathrm{p}}\left(\lambda(t), \beta(t)\right)$, which is a function of the pitch angle of the blades, $\beta(t)$, and the ratio between the speed of the blade tip and the wind speed, denoted tip-speed ratio, $\lambda(t)$. The aerodynamic torque applied to the rotor is given as:

$$T_{\mathrm{a}}(t) = \frac{1}{2\omega_{\mathrm{r}}(t)} \rho A v_{\mathrm{r}}^3(t) C_{\mathrm{p}}\left(\lambda(t), \beta(t)\right) \quad [\mathrm{Nm}] \qquad (1)$$

The coefficient C_{p} describes the aerodynamic efficiency of the rotor by the mapping illustrated in Fig. 1.

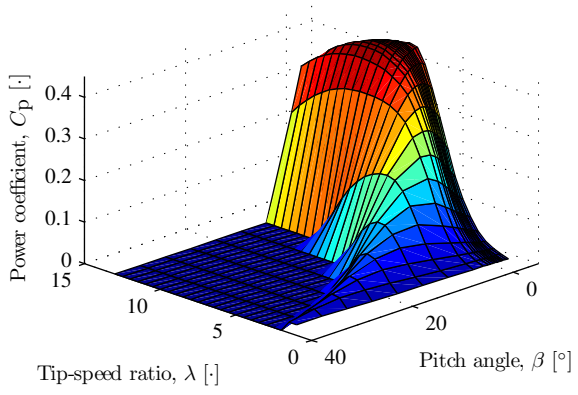

Fig. 1. Illustration of the power coefficient, C_{p}.

B. Drive Train Model

The drive train model consists of a low-speed shaft and a high-speed shaft having inertias J_{r} and J_{g}, and friction coefficients B_{r} and B_{g}. The shafts are interconnected by a transmission having gear ratio N_{g}, combined with torsion stiffness K_{dt}, and torsion damping B_{dt}. This results in a torsion angle, $\theta_{\Delta}(t)$, and a torque applied to the generator, $T_{\mathrm{g}}(t)$, at a speed $\omega_{\mathrm{g}}(t)$. The linear model is given as:

$$\begin{aligned} J_{\mathrm{r}}\dot{\omega}_{\mathrm{r}}(t) =& T_{\mathrm{a}}(t) + \frac{B_{\mathrm{dt}}}{N_{\mathrm{g}}}\omega_{\mathrm{g}}(t) \\ & - K_{\mathrm{dt}}\theta_{\Delta}(t) - (B_{\mathrm{dt}} + B_{\mathrm{r}})\omega_{\mathrm{r}}(t) \quad [\mathrm{Nm}] \end{aligned} \qquad (2)$$

$$\begin{aligned} J_{\mathrm{g}}\dot{\omega}_{\mathrm{g}}(t) =& \frac{K_{\mathrm{dt}}}{N_{\mathrm{g}}}\theta_{\Delta}(t) + \frac{B_{\mathrm{dt}}}{N_{\mathrm{g}}}\omega_{\mathrm{r}}(t) \\ & - \left(\frac{B_{\mathrm{dt}}}{N_{\mathrm{g}}^2} + B_{\mathrm{g}}\right)\omega_{\mathrm{g}}(t) - T_{\mathrm{g}}(t) \quad [\mathrm{Nm}] \end{aligned} \qquad (3)$$

$$\dot{\theta}_{\Delta}(t) = \omega_{\mathrm{r}}(t) - \frac{1}{N_{\mathrm{g}}}\omega_{\mathrm{g}}(t) \quad [\mathrm{rad/s}] \qquad (4)$$

C. Pitch System Model Including Fault Model

The considered wind turbine has a hydraulic pitch system that tracks a reference, $\beta_{\mathrm{ref}}(t)$, and is modeled as a second order system with a time delay, t_{d}. The natural frequency, ω_{n}, and damping ratio, ζ, specify the dynamics of the system:

$$\ddot{\beta}(t) = \text{-}2\zeta\omega_{\mathrm{n}}\dot{\beta}(t) - \omega_{\mathrm{n}}^2\beta(t) + \omega_{\mathrm{n}}^2\beta_{\mathrm{ref}}(t - t_{\mathrm{d}}) \quad [^{\circ}/\mathrm{s}^2] \qquad (5)$$

Besides the linear dynamics in (5), the model includes constraints on the slew rate and range of the pitch angle.

Fault Model: The air content of the hydraulic oil affects the damping and natural frequency of the pitch system, as described in (6). High air content is characterized as a fault, since it causes overshoot in the transient response of the pitch system due to a higher elasticity of the oil.

$$\zeta(t) = (1 - \alpha(t))\zeta_0 + \alpha(t)\zeta_{\mathrm{ha}} \quad [\cdot] \qquad (6a)$$

$$\omega_{\mathrm{n}}(t) = (1 - \alpha(t))\omega_{\mathrm{n},0} + \alpha(t)\omega_{\mathrm{n,ha}} \quad [\mathrm{rad/s}] \qquad (6b)$$

for $\alpha(t) \in [0, 1]$. The extreme values caused by $\alpha = 0$ and $\alpha = 1$ correspond to air content levels of 7% and 15% according to [7].

D. Generator and Converter Models

Electric power is generated by the generator, while a power converter interfaces the wind turbine generator output with the utility grid and controls the currents in the generator. The generator torque in (7) is adjusted by the reference $T_{\mathrm{g,ref}}(t)$. The converter dynamics are approximated by a first order system with time constant τ_{g} and time delay $t_{\mathrm{g,d}}$. Just as for the model of the pitch system, the slew rate and operating range of the generator torque are limited.

$$\dot{T}_{\mathrm{g}}(t) = \text{-}\frac{1}{\tau_{\mathrm{g}}}T_{\mathrm{g}}(t) + \frac{1}{\tau_{\mathrm{g}}}T_{\mathrm{g,ref}}(t - t_{\mathrm{g,d}}) \quad [\mathrm{Nm/s}] \qquad (7)$$

The power produced by the generator can be approximated from the mechanical power calculated in (8), where η_{g} denotes the efficiency of the generator, which is assumed constant.

$$P_{\mathrm{g}}(t) = \eta_{\mathrm{g}}\omega_{\mathrm{g}}(t)T_{\mathrm{g}}(t) \quad [\mathrm{W}] \qquad (8)$$

E. Assembled Model

The interconnection of the wind turbine sub-models is illustrated in Fig. 2. The disturbance input, $v_r(t)$, is provided by a wind model, where tower shadow and wind shear are modeled as in [9] using a turbulence model derived from the wind model in [10]. Furthermore, changes caused by swaying of the tower are added to the wind speed.

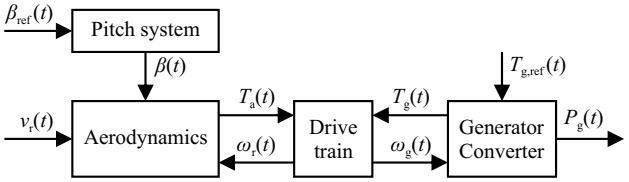

Fig. 2. Block diagram of the wind turbine model.

Available measurements are: generator torque, pitch angle, generator speed, and rotor speed; all sampled at a rate of 100 Hz. The measurement noise is modeled as zero-mean white Gaussian noise with the following standard deviations: $\sigma_{T_g} = 90$ Nm, $\sigma_\beta = 0.2°$, $\sigma_{\omega g} = 0.016$ rad/s, and $\sigma_{\omega r} = 0.025$ rad/s.

F. Model Parameters

The following parameters represent a realistic but fictitious wind turbine: $A = 10{,}387$ m^2, $\rho = 1.225$ kg/m^3, $B_r = 27.8$ kNm/(rad/s), $B_g = 3.034$ Nm/(rad/s), $B_{dt} = 945$ kNm/(rad/s), $J_r = 55 \cdot 10^6$ kgm^2, $J_g = 390$ kgm^2, $K_{dt} = 2.7$ GNm/rad, $N_g = 95$, $t_d = 10$ ms, $\omega_{n,0} = 11.11$ rad/s, $\zeta_0 = 0.6$ rad/s, $\omega_{n,ha} = 5.73$ rad/s, $\zeta_{ha} = 0.45$ rad/s, $t_{g,d} = 20$ ms, $\tau_g = 10$ ms, $\eta_g = 0.92$ with limitations $\dot{\beta} \in [\text{-}10°/\text{s}, \text{-}10°/\text{s}]$ and $\dot{T}_g \in [\text{-}50 \text{ MNm/s}, 50 \text{ MNm/s}]$.

III. CONTROLLER DESIGN

This section presents the LMI-based method for designing and synthesizing the active and passive fault-tolerant LPV controllers. The presented method extends the LPV controller design method [11] in which all parameter variations are measured, by allowing unmeasured parameter variations in a similar description. This design method is considered to be more intuitive than using scaling as in [5]. The considered wind turbine model has varying parameters caused by nonlinearities in the aerodynamic model along the nominal operating trajectory and variations in the pitch system dynamics due to the fault explained in Section II-C.

It was decided to design both an active and a passive fault-tolerant controller, to enable a comparison of the two solutions in terms of performance and design complexity. The difference between the structures of the two controllers is illustrated in Fig. 3. The generation of the scheduling parameters is explained in Section III-E.

As shown in the figure, the AFTC is dependent on a fault estimate, $\hat{\theta}_f(t)$, provided by the fault diagnosis system, while the PFTC only depends on the scheduling parameter, $\theta_{op}(t)$, indicating the nominal operating point of the wind turbine. The extra degree of freedom added by allowing the AFTC to adapt in case of a fault may enable less conservatism.

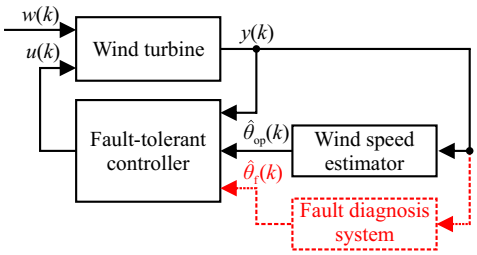

Fig. 3. Block diagram of the controller structures. The black boxes are common to both controllers, while the red dashed box illustrates the fault diagnosis system required for the AFTC.

However, if the fault diagnosis system behaves incorrectly, the AFTC is affected in an undesirable manner. This risk is eliminated for the PFTC, since it is designed to be resilient against the fault without depending on the fault diagnosis system.

Notice that the AFTC is in fact a conventional LPV controller, scheduled on $\theta_{op}(t)$ and $\theta_f(t)$; the reason for denoting it an active fault-tolerant controller arises from the origin of the scheduling parameters. Throughout this paper $\theta(t)$ represents the measured parameter variations and $\Delta(t)$ the unmeasured parameter variations. Correspondingly, for the cases under consideration:

$$\text{AFTC}: \quad \theta_1(t) = \theta_{op}(t) \quad \text{and} \quad \theta_2(t) = \theta_f(t) \tag{9a}$$

$$\text{PFTC}: \quad \theta_1(t) = \theta_{op}(t) \quad \text{and} \quad \Delta_1(t) = \theta_f(t) \tag{9b}$$

The AFTC is designed using the LPV controller design method described in [11]. This method assumes output feedback, which suits the considered problem well, since the state vector is only partially measured. To enable design of a PFTC, the description in [11] is extended in this paper, by introducing unmeasured parameter variations.

A. System and Controller Description

The model of the plant is given by the general LPV system description shown below, where the subscripts θ and Δ are used as shorthand notation to indicate that the matrices depend on $\theta(t)$ and $\Delta(t)$. This shorthand notation is utilized throughout this paper. Note that $z(t)$ is the performance output vector and $w(t)$ is the disturbance input vector.

$$\dot{x}(t) = A_{\theta\Delta}x(t) + B_{1\theta\Delta}w(t) + B_{2\theta\Delta}u(t) \tag{10a}$$

$$z(t) = C_{1\theta\Delta}x(t) + D_{11\theta\Delta}w(t) + D_{12\theta\Delta}u(t) \tag{10b}$$

$$y(t) = C_{2\theta\Delta}x(t) + D_{21\theta\Delta}w(t) + D_{22\theta\Delta}u(t) \tag{10c}$$

The unmeasured parameter vector Δ is empty for the active fault-tolerant controller, since all scheduling parameters are measured, as indicated in (9a).

To reduce the number of matrix inequalities in the optimization problem used to compute the controller matrices, an affine parameter description was adapted with some restrictions on the matrices in terms of dependency on the parameter variations, simplifying the general case explained in [11]. The system description is shown in (11), where n_θ

is the number of measured parameters and n_Δ is the number of unmeasured parameters.

$$\begin{bmatrix} A_{\theta\Delta} & B_{1\theta\Delta} & B_{2\theta\Delta} \\ C_{1\theta\Delta} & D_{11\theta\Delta} & D_{12\theta\Delta} \\ C_{2\theta\Delta} & D_{21\theta\Delta} & D_{22\theta\Delta} \end{bmatrix} = \begin{bmatrix} A_0 & B_{1,0} & B_{2,0} \\ C_{1,0} & D_{11,0} & D_{12,0} \\ C_{2,0} & D_{21,0} & 0 \end{bmatrix} + \sum_{i=1}^{n_\theta} \theta_i \begin{bmatrix} A_i^\theta & B_{1,i}^\theta & 0 \\ C_{1,i}^\theta & D_{11,i}^\theta & 0 \\ 0 & 0 & 0 \end{bmatrix} + \sum_{j=1}^{n_\Delta} \Delta_j \begin{bmatrix} A_j^\Delta & 0 & 0 \\ 0 & 0 & 0 \\ 0 & 0 & 0 \end{bmatrix} \quad (11)$$

For convenience the matrices A_θ and A_Δ^{lin} are defined below, describing the measured and unmeasured parameter variations.

$$A_{\theta\Delta} = \underbrace{A_0 + \sum_{i=1}^{n_\theta} \theta_i A_i^\theta}_{A_\theta} + \underbrace{\sum_{j=1}^{n_\Delta} \Delta_j A_j^\Delta}_{A_\Delta^{\text{lin}}} \quad (12)$$

Notice that the AFTC has no unmeasured parameters, and that the following relations hold:

$$\text{AFTC}: \quad A_{\theta\Delta} = A_\theta \quad (13a)$$

$$\text{PFTC}: \quad A_{\theta\Delta} = A_\theta + A_\Delta^{\text{lin}} \quad (13b)$$

Both controllers share the controller description in (14), where the controller matrices are dependent on the measured parameters, $\theta(t)$.

$$\dot{x}_\text{c}(t) = A_{\text{c}\theta} x_\text{c}(t) + B_{\text{c}\theta} y(t) \quad (14a)$$

$$u(t) = C_{\text{c}\theta} x_\text{c}(t) + D_{\text{c}\theta} y(t) \quad (14b)$$

B. LPV Controller Design Method

From the description of the system and the LPV controller, the design task is to find a parameter-dependent quadratic stable closed-loop system, which minimizes the induced $\mathcal{L}_2$-norm between the disturbance input, $w(t)$, and the performance output, $z(t)$. This can be accomplished by finding parameter-dependent Lyapunov functions, as explained in the following theorem [5] originating from [11]:

Theorem 1: Given a closed-loop system governed by the parameter-dependent matrices $A_{\text{cl}\theta\Delta}, B_{\text{cl}\theta}, C_{\text{cl}\theta}, D_{\text{cl}\theta}$ with $(\theta, \dot{\theta}, \Delta, \dot{\Delta}) \in \Theta \times \mathcal{V} \times \mathcal{D} \times \mathcal{U}$, suppose that there exists a differentiable symmetric function $X_{\text{cl}\theta}$ such that $X_{\text{cl}\theta} > 0$ and

$$\begin{bmatrix} \dot{X}_{\text{cl}\theta} + A_{\text{cl}\theta\Delta}^\text{T} X_{\text{cl}\theta} + X_{\text{cl}\theta} A_{\text{cl}\theta\Delta} & X_{\text{cl}\theta} B_{\text{cl}\theta} & C_{\text{cl}\theta}^\text{T} \\ B_{\text{cl}\theta}^\text{T} X_{\text{cl}\theta} & -\gamma I & D_{\text{cl}\theta}^\text{T} \\ C_{\text{cl}\theta} & D_{\text{cl}\theta} & -\gamma I \end{bmatrix} < 0 \quad (15)$$

for all $(\theta, \dot{\theta}, \Delta, \dot{\Delta}) \in \Theta \times \mathcal{V} \times \mathcal{D} \times \mathcal{U}$. Then,

1) *the function $A_{\text{cl}\theta\Delta}$ is PDQ stable over $\Theta \times \mathcal{D}$ and,*
2) *the induced $\mathcal{L}_2$-norm of the operator T_{zw} is bounded by $\gamma > 0$ (i.e. $||T_{zw}||_{i,2} < \gamma$).*

Note that a bound $\gamma > 0$ on $||T_{zw}||_{i,2}$ means that

$$\int_0^\infty z^\text{T}(\tau) z(\tau) d\tau < \gamma^2 \int_0^\infty w^\text{T}(\tau) w(\tau) d\tau \quad (16)$$

Theorem 1 cannot be utilized directly for controller design, since the closed-loop system matrices are unknown. To form an appropriate design problem, which can be solved using convex optimization, some auxiliary controller matrices are defined as shown in (17). Notice that '*' is inferred by symmetry and that the bold symbols are unknown matrices in the design problem.

$$\hat{\boldsymbol{A}}_\theta = N_\theta A_{\text{c}\theta} M_\theta^\text{T} - \boldsymbol{X}_\theta \dot{\boldsymbol{Y}}_\theta - N_\theta \dot{M}_\theta^\text{T} + \boldsymbol{X}_\theta B_2 C_{\text{c}\theta} M_\theta^\text{T} + N_\theta B_{\text{c}\theta} C_2 \boldsymbol{Y}_\theta + \boldsymbol{X}_\theta \left(A_\theta + B_2 D_{\text{c}\theta} C_2\right) \boldsymbol{Y}_\theta \quad (17a)$$

$$\hat{\boldsymbol{B}}_\theta = N_\theta B_{\text{c}\theta} + \boldsymbol{X}_\theta B_2 D_{\text{c}\theta} \quad (17b)$$

$$\hat{\boldsymbol{C}}_\theta = C_{\text{c}\theta} M_\theta^\text{T} + D_{\text{c}\theta} C_2 \boldsymbol{Y}_\theta \quad (17c)$$

$$\hat{\boldsymbol{D}}_\theta = D_{\text{c}\theta} \quad (17d)$$

Due to the assumption of an affine parameter description, the Lyapunov matrices, $\boldsymbol{X}_\theta$ and $\boldsymbol{Y}_\theta$, and auxiliary matrices, $\hat{\boldsymbol{A}}_\theta, \hat{\boldsymbol{B}}_\theta, \hat{\boldsymbol{C}}_\theta, \hat{\boldsymbol{D}}_\theta$, in (17) are described using an affine description:

$$\boldsymbol{X}_\theta = \boldsymbol{X}_0 + \sum_{i=1}^{n_\theta} \theta_i \boldsymbol{X}_i \qquad \boldsymbol{Y}_\theta = \boldsymbol{Y}_0 + \sum_{i=1}^{n_\theta} \theta_i \boldsymbol{Y}_i \quad (18a)$$

$$\hat{\boldsymbol{A}}_\theta = \hat{\boldsymbol{A}}_0 + \sum_{i=1}^{n_\theta} \theta_i \hat{\boldsymbol{A}}_i \qquad \hat{\boldsymbol{B}}_\theta = \hat{\boldsymbol{B}}_0 + \sum_{i=1}^{n_\theta} \theta_i \hat{\boldsymbol{B}}_i \quad (18b)$$

$$\hat{\boldsymbol{C}}_\theta = \hat{\boldsymbol{C}}_0 + \sum_{i=1}^{n_\theta} \theta_i \hat{\boldsymbol{C}}_i \qquad \hat{\boldsymbol{D}}_\theta = \hat{\boldsymbol{D}}_0 + \sum_{i=1}^{n_\theta} \theta_i \hat{\boldsymbol{D}}_i \quad (18c)$$

From (15), (17), and (18), Theorem 1 is reformulated into:

Theorem 2: Given the open-loop LPV system in (10) *with matrices defined in* (11)*, suppose that there exists two parameter-dependent symmetric matrices $\boldsymbol{X}_\theta$ and $\boldsymbol{Y}_\theta$ and four parameter-dependent matrices $\hat{\boldsymbol{A}}_\theta$, $\hat{\boldsymbol{B}}_\theta$, $\hat{\boldsymbol{C}}_\theta$, $\hat{\boldsymbol{D}}_\theta$ such that for all $(\theta, \dot{\theta}, \Delta, \dot{\Delta}) \in \Theta \times \mathcal{V} \times \mathcal{D} \times \mathcal{U}$,*

$$\begin{bmatrix} \phi_{11} & * & * & * \\ \phi_{21} & \phi_{22} & * & * \\ (\boldsymbol{X}_\theta B_{1\theta} + \hat{\boldsymbol{B}}_\theta D_{21})^\text{T} & \phi_{32} & \text{-}\gamma I_{n_w} & * \\ C_{1\theta} + D_{12} \hat{\boldsymbol{D}}_\theta C_2 & \phi_{42} & \phi_{43} & \text{-}\gamma I_{n_z} \end{bmatrix} < 0 \quad (19a)$$

$$\phi_{11} = \dot{\boldsymbol{X}}_\theta + \boldsymbol{X}_\theta A_{\theta\Delta} + \hat{\boldsymbol{B}}_\theta C_2 + (*)$$

$$\phi_{21} = \hat{\boldsymbol{A}}_\theta^\text{T} + \boldsymbol{Y}_\theta \left(A_\Delta^{\text{lin}}\right)^\text{T} \boldsymbol{X}_\theta + A_{\theta\Delta} + B_2 \hat{\boldsymbol{D}}_\theta C_2$$

$$\phi_{22} = \text{-}\dot{\boldsymbol{Y}}_\theta + A_{\theta\Delta} \boldsymbol{Y}_\theta + B_2 \hat{\boldsymbol{C}}_\theta + (*)$$

$$\phi_{32} = (B_{1\theta} + B_2 \hat{\boldsymbol{D}}_\theta D_{21})^\text{T}$$

$$\phi_{42} = C_{1\theta} \boldsymbol{Y}_\theta + D_{12} \hat{\boldsymbol{C}}_\theta$$

$$\phi_{43} = D_{11\theta} + D_{12} \hat{\boldsymbol{D}}_\theta D_{21}$$

$$\begin{bmatrix} \boldsymbol{X}_\theta & I \\ I & \boldsymbol{Y}_\theta \end{bmatrix} > 0 \quad (19b)$$

Then, there exists a controller of the form in (14) *such that*

1) *the closed-loop system is PDQ stable over $\Theta \times \mathcal{D}$ and,*
2) *the induced $\mathcal{L}_2$-norm of the operator T_{zw} is bounded by $\gamma > 0$ (i.e. $||T_{zw}||_{i,2} < \gamma$).*

It is only necessary to test the matrix inequalities (19a)-(19b) in the vertices of the parameter space, Δ_{vex}, if the following additional constraint is satisfied:

$$\begin{bmatrix} \boldsymbol{X}_i A_i^\theta + (*) & * & * & * \\ \boldsymbol{Y}_i \left(A_\Delta^{\text{lin}}\right)^{\mathrm{T}} \boldsymbol{X}_i & A_i^\theta \boldsymbol{Y}_i + (*) & * & * \\ \left(B_{1,i}^\theta\right)^{\mathrm{T}} \boldsymbol{X}_i & 0 & 0 & * \\ 0 & C_{1,i}^\theta \boldsymbol{Y}_i & 0 & 0 \end{bmatrix} \geq 0 \tag{19c}$$

for $i = 1 \dots n_\theta$ *and* $\Delta \in \Delta_{\text{vex}}$.

It appears from the structure of (19c) that $\boldsymbol{X}_i$ should be in the null space of $\left(B_{1,i}^\theta\right)^{\mathrm{T}}$ and $\boldsymbol{Y}_i$ should be in the null space of $C_{1,i}^\theta$ to avoid getting an indefinite matrix. Note that usually $\boldsymbol{X}_\theta$ or $\boldsymbol{Y}_\theta$ is independent of $\theta(t)$, i.e. either $\boldsymbol{X}_i$ or $\boldsymbol{Y}_i$ is a zero matrix.

For the active fault-tolerant controller, A_Δ^{lin} is a zero matrix, turning the optimization problem into an LMI-based optimization problem, since the term $\boldsymbol{Y}_\theta \left(A_\Delta^{\text{lin}}\right)^{\mathrm{T}} \boldsymbol{X}_\theta$ disappears in ϕ_{12} and ϕ_{21}. This means that it is a convex optimization problem; hence, the controller giving the smallest γ can be found. In contrast, the optimization problem for the PFTC is based on bilinear matrix inequalities (BMIs) due to non-zero elements in A_Δ^{lin}; hence, some additional work must be done to solve this problem.

C. Solving the Optimization Problem for the Passive Fault-Tolerant Controller

To solve the BMI-based optimization problem for the PFTC a two-step procedure is proposed inspired by [12], where the projection lemma, provided hereafter, is utilized to write two necessary conditions for the BMI.

Lemma 1: Given a symmetric matrix Ω and matrices $\mathcal{B}$ and $\mathcal{C}$ of compatible dimensions, there exists a matrix $\mathcal{L}$ such that $\Omega + \mathcal{B}\mathcal{L}\mathcal{C} + (\mathcal{B}\mathcal{L}\mathcal{C})^{\mathrm{T}} < 0$ if and only if $\mathcal{B}_\perp^{\mathrm{T}} \Omega \mathcal{B}_\perp < 0$ and $(\mathcal{C}^{\mathrm{T}})_\perp^{\mathrm{T}} \Omega (\mathcal{C}^{\mathrm{T}})_\perp < 0$, where $\mathcal{B}_\perp$ is defined as a basis for the null space of $\mathcal{B}^{\mathrm{T}}$.

One of the necessary conditions (20) and (21) must be solved before solving (19) to provide half the unknown variables; hence, making (19) linear in the unknown variables. Notice that the two steps are dependent and that the final result is affected by the initialization of the optimization problem. The two necessary conditions for the BMI are:

Necessary Condition for $\boldsymbol{X}_\theta$*:*

$$\begin{bmatrix} \phi_{11} & * & * \\ (\boldsymbol{X}_\theta B_{1\theta} + \hat{\boldsymbol{B}}_\theta D_{21})^{\mathrm{T}} & \text{-}\gamma I_{n_w} & * \\ C_{1\theta} + D_{12} \hat{\boldsymbol{D}}_\theta C_2 & D_{11\theta} + D_{12} \hat{\boldsymbol{D}}_\theta D_{21} & \text{-}\gamma I_{n_z} \end{bmatrix} < 0 \tag{20a}$$

for all $\theta \in \theta_{\text{vex}}$, $\Delta \in \Delta_{\text{vex}}$, $\dot{\theta} \in \dot{\theta}_{\text{vex}}$, *and*

$$\begin{bmatrix} \boldsymbol{X}_i A_i^\theta + (*) & * & * \\ \left(B_{1,i}^\theta\right)^{\mathrm{T}} \boldsymbol{X}_i & 0 & * \\ 0 & 0 & 0 \end{bmatrix} \geq 0 \tag{20b}$$

for $i = 1 \dots n_\theta$.

Necessary Condition for $\boldsymbol{Y}_\theta$*:*

$$\begin{bmatrix} \phi_{22} & * & * \\ (B_{1\theta} + B_2 \hat{\boldsymbol{D}}_\theta D_{21})^{\mathrm{T}} & \text{-}\gamma I_{n_w} & * \\ C_{1\theta} \boldsymbol{Y}_\theta + D_{12} \hat{\boldsymbol{C}}_\theta & D_{11\theta} + D_{12} \hat{\boldsymbol{D}}_\theta D_{21} & \text{-}\gamma I_{n_z} \end{bmatrix} < 0 \tag{21a}$$

for all $\theta \in \theta_{\text{vex}}$, $\Delta \in \Delta_{\text{vex}}$, $\dot{\theta} \in \dot{\theta}_{\text{vex}}$, *and*

$$\begin{bmatrix} A_i^\theta \boldsymbol{Y}_i + (*) & * & * \\ 0 & 0 & * \\ C_{1,i}^\theta \boldsymbol{Y}_i & 0 & 0 \end{bmatrix} \geq 0 \tag{21b}$$

for $i = 1 \dots n_\theta$.

A robust controller is designed to guarantee the same performance in the entire parameter space, whereas a reliable controller, which is considered in this paper, is designed to guarantee higher performance in the normal case than in the faulty case. This is achieved by using different γ values for the normal and faulty systems. Between the two vertices, the guaranteed performance follows graceful degradation according to $\gamma = \frac{\gamma_{\text{n}} \gamma_{\text{f}}}{\gamma_{\text{n}} \alpha + \gamma_{\text{f}} (1-\alpha)}$, where α indicates the state of the system between 0 (faulty, γ_{f}) and 1 (normal, γ_{n}).

D. Controller Synthesis

When the optimization problem is solved, the following synthesis procedure is used to calculate the controller matrices at each sample time:

1) Compute $\hat{\boldsymbol{A}}_\theta$, $\hat{\boldsymbol{B}}_\theta$, $\hat{\boldsymbol{C}}_\theta$, $\hat{\boldsymbol{D}}_\theta$, $\boldsymbol{X}_\theta$, and $\boldsymbol{Y}_\theta$ using the measured value of $\theta(t)$.
2) Find M_θ and N_θ by solving the factorization problem:
$$I - \boldsymbol{X}_\theta \boldsymbol{Y}_\theta = N_\theta M_\theta^{\mathrm{T}} \tag{22}$$
3) Compute $A_{\text{c}\theta\dot{\theta}}$, $B_{\text{c}\theta}$, $C_{\text{c}\theta}$, and $D_{\text{c}\theta}$ from the equations:
$$\begin{aligned} A_{\text{c}\theta\dot{\theta}} = N_\theta^{-1} \Big(& \boldsymbol{X}_\theta \dot{\boldsymbol{Y}}_\theta + N_\theta \dot{M}_\theta^{\mathrm{T}} + \hat{\boldsymbol{A}}_\theta - \hat{\boldsymbol{B}}_\theta C_2 \boldsymbol{Y}_\theta \\ & - \boldsymbol{X}_\theta \left(A_\theta - B_2 \hat{\boldsymbol{D}}_\theta C_2\right) \boldsymbol{Y}_\theta - \boldsymbol{X}_\theta B_2 \hat{\boldsymbol{C}}_\theta \Big) M_\theta^{-\mathrm{T}} \end{aligned} \tag{23a}$$
$$B_{\text{c}\theta} = N_\theta^{-1} \left(\hat{\boldsymbol{B}}_\theta - \boldsymbol{X}_\theta B_2 \hat{\boldsymbol{D}}_\theta\right) \tag{23b}$$
$$C_{\text{c}\theta} = \left(\hat{\boldsymbol{C}}_\theta - \hat{\boldsymbol{D}}_\theta C_2 \boldsymbol{Y}_\theta\right) M_\theta^{-\mathrm{T}} \tag{23c}$$
$$D_{\text{c}\theta} = \hat{\boldsymbol{D}}_\theta \tag{23d}$$

According to [11] either $\boldsymbol{X}_\theta$ or $\boldsymbol{Y}_\theta$ must be held constant if the controller should be synthesized without measuring $\dot{\theta}(t)$. Furthermore, if N_θ and M_θ are chosen according to Table I in [11], dependencies of $\dot{\theta}(t)$ can be removed from the calculation of $A_{\text{c}\theta}$ resulting in (24).

$$\begin{aligned} A_{\text{c}\theta} = N_\theta^{-1} \Big(& \hat{\boldsymbol{A}}_\theta - \hat{\boldsymbol{B}}_\theta C_2 \boldsymbol{Y}_\theta - \boldsymbol{X}_\theta \left(A_\theta - B_2 \hat{\boldsymbol{D}}_\theta C_2\right) \boldsymbol{Y}_\theta \\ & - \boldsymbol{X}_\theta B_2 \hat{\boldsymbol{C}}_\theta \Big) M_\theta^{-\mathrm{T}} \end{aligned} \tag{24}$$

This finalizes the procedure for realizing the controllers. The last part of this section applies the design method to the cases under consideration.

E. Computation of Controllers

To formulate the optimization problems utilized in the controller design, an affine system description in the scheduling parameters was first derived. Secondly, a performance specification was composed. Finally, the optimization problem for each of the controllers was solved.

Scheduling Parameters: Since the two controller design problems rely on affine system descriptions in the parameters $\theta_{\mathrm{op}}(t)$ and $\theta_{\mathrm{f}}(t)$, an affine system description is introduced in this subsection, including both the parameter variations in the operating point and the parameter variations introduced by the fault. The range and rate bounds of the scheduling parameters are included.

The instantaneous partial derivatives of the aerodynamic torque are part of the linearized model and change along the nominal operating trajectory. These changes were approximated using an affine description in the wind speed; hence, $\theta_{\mathrm{op}}(t) = v_{\mathrm{r}}(t)$. It was chosen to select wind speeds in the interval between 18 m/s and 25 m/s as the operating range, which makes up the majority of the full load region. By inspecting the output of the wind model, the rate bounds of $v_{\mathrm{r}}(t)$ were approximated to be -2 m/s^2 and 2 m/s^2.

Since wind turbines only provide a poor wind measurement and only of a point wind speed, not being representative for the effective wind speed, it had to be estimated. To estimate the wind speed an effective wind speed estimator was designed according to the method described in [13].

With respect to the considered fault, the damping factor, ζ, and natural frequency, ω_{n}, change according to the air content of the pitch system. The introduced changes in the system equations were approximated with an affine function in ω_{n}^2; hence, $\theta_{\mathrm{f}}(t) = \omega_{\mathrm{n}}^2(t)$. The range of $\omega_{\mathrm{n}}^2(t)$ is between $(5.73 \text{ rad/s})^2$ and $(11.11 \text{ rad/s})^2$. Since the dynamics of the fault is much slower than the dynamics of the system, the rate bound on $\theta_{\mathrm{f}}(t)$ was set to zero in the controller design.

The scheduling parameter $\omega_{\mathrm{n}}^2(t)$ was not measured and had to be estimated for the AFTC. The method utilized for this parameter estimation is explained in [14]. The parameter estimation method was based on a multiple-model estimation using an extended Kalman filter, which relies on the measured pitch angle of all three blades.

Performance Specification: The performance specifications for the active and passive LPV controllers were identical, in order to enable a direct comparison of their performance. The specification was based on a mixed sensitivity description, where it was chosen to specify sensitivity and control sensitivity. The mixed sensitivity description was implemented as shown in Fig. 4, where $W_{\mathrm{S}}(s)$ is the sensitivity filter and $W_{\mathrm{M}}(s)$ is the control sensitivity filter.

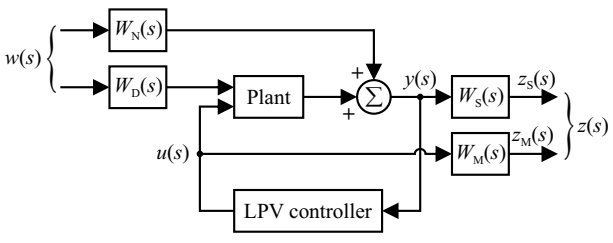

Fig. 4. Block diagram of the mixed sensitivity description.

In addition to the sensitivity filters, the input disturbance filter, $W_{\mathrm{D}}(s)$, band limits the exogenous input in the design and $W_{\mathrm{N}}(s)$ adds measurement noise to the system outputs.

$W_{\mathrm{S}}(s)$ stresses the importance of the low-frequency components of the generator speed error. It has a pole at the origin to ensure integral action in the controllers to eliminate steady-state errors on the tracking of the generator speed. $W_{\mathrm{M}}(s)$ weights the control effort with the aim of penalizing fast pitch angle variations. The weighted performance measures appear in (25) and the filters are specified in (26)-(27).

$$z(s) = \begin{bmatrix} W_{\mathrm{S}}(s) & 0 \\ 0 & W_{\mathrm{M}}(s) \end{bmatrix} \begin{bmatrix} \omega_{\mathrm{g,e}}(s) \\ \beta_{\mathrm{ref}}(s) \end{bmatrix} \tag{25}$$

$$W_{\mathrm{S}}(s) = k_{\mathrm{S}} \frac{1}{s}, \quad W_{\mathrm{M}}(s) = k_{\mathrm{M}} \frac{s}{s/(10\omega_{3\mathrm{P}}) + 1} \tag{26}$$

$$W_{\mathrm{D}}(s) = \frac{1}{s/(1.5\omega_{3\mathrm{P}}) + 1} \tag{27}$$

Solving the Optimization Problems: The optimization problems were set up in YALMIP and solved using SeDuMi, based on balanced state-space realizations. To decide whether $\boldsymbol{X}_\theta$ or $\boldsymbol{Y}_\theta$ should be held constant, the optimization problems were solved using all possible combinations of constant and parameter-dependent Lyapunov matrices, $\boldsymbol{X}_\theta$ and $\boldsymbol{Y}_\theta$. For both controllers the smallest γ values were obtained by choosing $\boldsymbol{X}_\theta$ to be constant and $\boldsymbol{Y}_\theta$ to be dependent on $\theta(t)$.

Since the optimization problem for the PFTC can be initialized in multiple ways, it was determined based on experiments that the best disturbance attenuation was obtained when using the necessary condition in (20) to initialize the optimization problem shown in (19). For the PFTC $\gamma_{\mathrm{f}} = 1$ was used in the optimization problem to degrade the performance for the nominal situation as little as possible, resulting in $\gamma_{\mathrm{n}} = 0.541$. Solving the AFTC resulted in $\gamma = 0.556$.

This finalizes the controller design. In the next section simulation results of the two control systems are presented.

IV. SIMULATION RESULTS

Simulations were conducted in MATLAB Simulink using the non-linear model provided in Section II to determine the performance of the active and passive fault-tolerant controllers during fault-free and faulty operation. To compare performance to a controller, which is designed using classical principles and corresponds to a simplified wind turbine controller, a PI-controller was used as reference.

Comparison of the Active and Passive LPV Controllers and the Reference Controller

To compare the performance of the fault-tolerant controllers, simulations of duration 5,000 s were conducted both with the normal air content level of 7% and at a level of 15%, at wind speeds ranging from 18 m/s to 25 m/s. Simulations at intermediate air content levels were also conducted, but are omitted due to space restrictions.

The first 50 s of the simulations are shown in Fig. 5. The gray lines show the simulation results of the reference controller, which is not designed to handle increased air content in the pitch system and therefore performs poorly in this situation. The performance measures obtained for the entire simulations are stated in Table I.

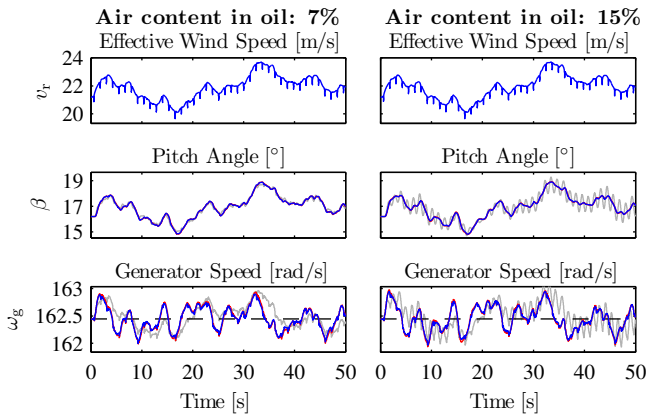

Fig. 5. Simulation results of the AFTC (blue) and the PFTC (red) conducted at both normal and high air content levels in the oil. The behaviors of the fault-tolerant controllers can be compared to the operation of the reference controller (gray).

TABLE I

Speed tracking errors and pitch actuator usage, normalized to the performance of the AFTC. The numbers in parentheses denote normalization with respect to the AFTC at 15% air in the oil.

Controller	$\int_0^t(\omega_{g,e}(\tau))^2\,d\tau$	$\int_0^t \dot{\beta}^2(\tau)\,d\tau$
	Air content in oil: 7%	
AFTC	1.00	1.00
PFTC	1.18	0.94
Reference	1.59	1.17
	Air content in oil: 15%	
AFTC	1.19 (1.00)	1.10 (1.00)
PFTC	1.29 (1.08)	1.14 (1.03)
Reference	1.79 (1.50)	10.71 (9.67)

Since the fault-tolerant controllers are designed based on the same structure and specification, they behave similarly, which is apparent from Fig. 5. However, the active fault-tolerant controller is better at tracking the reference speed, especially in the fault-free case. The reason is that this controller is less conservative, since controller adaptation is offered based on the fault diagnosis signal. In line with this explanation it is further concluded that the passive fault-tolerant controller has less actuator usage in the fault-free case than the active fault-tolerant controller.

The performance measures stated for the reference controller in Table I show that the fault-tolerant controllers are superior to the reference controller in both performance measures, which emphasizes the advantages of a multi-variable LPV controller compared to a PI controller.

V. CONCLUSION

This paper addresses the design of an active and a passive fault-tolerant LPV controller for a wind turbine operating in the full load region with a fault in the pitch system. The controllers handle both the parameter variations along the nominal operating trajectory and the parameter variations introduced by the fault in the hydraulic pitch system, caused by high air content in the oil.

Simulation show that the AFTC performs somewhat better than the PFTC, especially when a fault is present. This is expected, since the AFTC is allowed to adapt to the behavior of the faulty pitch system. From the simulations we see the importance of taking faults into consideration, since a reference controller designed for the nominal system becomes unstable when the fault is introduced.

Since the PFTC does not rely on a fault diagnosis algorithm, it has a simple structure and has no risk of making false decisions. However, the optimization problem for the PFTC involves solving BMIs instead of LMIs, making it far more difficult to solve, since it is non-convex and does not ensure convergence towards the global minimum. The AFTC however is solved using a convex optimization approach, and is guaranteed to provide the optimum controller in terms of maximum disturbance attenuation.

In general, an AFTC should be used on systems for which a fault diagnosis system can be designed to be sufficiently fast with a low risk of making false decisions. If a fault changes the system behavior significantly, then an AFTC should also be applied because controller adaptation will have a large impact on performance. A PFTC should be favored when faults are difficult to diagnose or there is zero tolerance for false decisions in the fault diagnosis system.

REFERENCES

[1] Global Wind Energy Council, "Global Wind 2008 Report", 2009.

[2] K. Hammerum, "A fatigue approach to wind turbine control", *Master's Thesis*, Technical University of Denmark, 2006

[3] C. Sloth, T. Esbensen, M.O.K. Niss, J. Stoustrup, and P.F. Odgaard, "Robust LMI-Based Control of Wind Turbines with Parametric Uncertainties", In *Proceedings of the 3rd IEEE Multi-conference on Systems and Control*, Saint Petersburg, Russia, JUL 2009.

[4] M.O.K. Niss, T. Esbensen, C. Sloth, J. Stoustrup, and P.F. Odgaard, "A Youla-Kucera approach to Gain-Scheduling with Application to Wind Turbine Control", In *Proceedings of the 3rd IEEE Multi-conference on Systems and Control*, Saint Petersburg, Russia, JUL 2009.

[5] F.D. Bianchi and H.D. Battista and R.J. Mantz, "Wind Turbine Control Systems: Principles, Modelling and Gain Scheduling Design", Springer, ISBN: 1-84628-492-9, 2007.

[6] K.Z. Østergaard, "Robust, Gain-Scheduled Control of Wind Turbines", *PhD Thesis*, Aalborg University, 2008, http://vbn.aau.dk/fbspretrieve/14618811/thesis_KZ__300608.pdf.

[7] P.F. Odgaard, J. Stoustrup and M. Kinnaert, "Fault Tolerant Control of Wind Turbines - a benchmark model", In *Proceedings of the 7th IFAC Symposium on Fault Detection, Supervision and Safety of Technical Processes*, Barcelona, Spain, JUN 2009, pp. 155-160.

[8] T. Esbensen and C. Sloth, "Fault Diagnosis and Fault-Tolerant Control of Wind Turbines", *Master's Thesis*, Aalborg University, 2009, http://projekter.aau.dk/projekter/fbspretrieve/19664716/Fault_Diagnosis_and_Fault-Tolerant_Control_of_Wind_Turbines.pdf.

[9] D.S.L. Dolan and P.W. Lehn, "Simulation Model of Wind Turbine 3p Torque Oscillations due to Wind Shear and Tower Shadow", *IEEE Trans. on Energy Conversion*, 21(3), SEP 2006, pp. 717-724.

[10] Aalborg University and Risø National Laboratory, "Wind Turbine Blockset", 2005.

[11] P. Apkarian and R.J. Adams, "Advanced Gain-Scheduling Techniques for Uncertain Systems", *IEEE Transactions on Control Systems Technology*, vol. 6, no. 1, JAN 1998, pp. 21-32.

[12] F. Jabbari, "Output Feedback Controllers for Systems with Structured Uncertainties", *IEEE Transactions on Automatic Control*, vol. 42, no. 5, MAY 1997, pp. 715-719.

[13] K.Z. Østergaard, P. Brath, and J. Stoustrup, "Estimation of effective wind speed", *Journal of Physics: Conf. Series*, vol. 75, 2007.

[14] R. Hallouzi, "Multiple-Model Based Diagnosis for Adaptive Fault-Tolerant Control", *PhD Thesis*, TU Delft, 2008, pp. 37-38, 63-64.